

Figure.2 A distributed bandpass transmission line section

The model of the distributed BP transmission line section is shown in Figure 2. By using the model, the characteristic impedance (Z_0) and propagation constant (γ) formulas of the BP line can be easily obtained, as made in transmission line analysis [7]. After the routine analysis, it can be observed that Z_0 is constant under the condition of

$$L_1 C_1 = L_2 C_2 \quad (2)$$

and for this case, we obtain the equations of

$$Z_0 = \sqrt{\frac{L_1}{C_2}} = \sqrt{\frac{L_2}{C_1}} \quad (3)$$

$$\gamma = j \frac{\omega^2 L_2 C_2 - 1}{\omega} \frac{1}{\sqrt{L_2 C_1}} \quad (4)$$

From Eqs. (4) and (2), it can be easily observed that $\gamma=0$ for

$$\omega_0 = \sqrt{\frac{1}{L_2 C_2}} = \sqrt{\frac{1}{L_1 C_1}} \quad (5)$$

As explained above, two different BP structure have been presented in the literature. Figure 2 shows the second BP structure [6]. In the previously used BP structure [5], a shunt inductance (L_2) is used in addition to the lowpass case and C_1 is not used. In that case, Eq. (3) changes to

$$Z_0 = \sqrt{\frac{Z}{Y}} = \sqrt{\frac{sL_1}{\frac{1}{sL_2} + sC_2}} \quad (6)$$

It is easily seen from this equation that Z_0 does not remain constant with frequency and approaches $\sqrt{L_1/C_2}$ as frequency increases. Therefore, the gain-frequency performance of a DA with the structure is poor at low frequencies. As a result, bandwidth of a DA with the previously used BP structure is narrower than that of a LP-DA (CDA) using the same active component.

III. BASIC ANALYSIS AND DESIGN OF THE BPDA

As in the lowpass case, while changing the distributed BP structure used in this work into lumped BP structure, we see that Eq. (3) and Eq. (4) can be used for Z_0 and γ in a limited band whose geometric center frequency is ω_0 given in Eq (5).

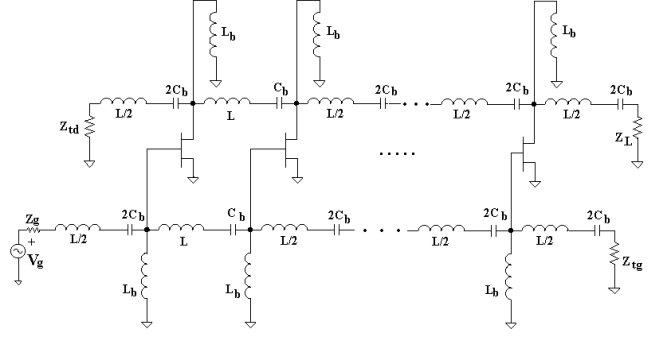


Figure.3 A DA with the bandpass filter structure

The schematic diagram of the BP-DA is given in Figure 3. It can be seen from passive filter transformations [8] that the BP structure, as in the LP case, has a bandwidth of

$$BW = 1/\pi \sqrt{L_1 C_2} \quad (7)$$

If ω_L is the lower limit and ω_U is the upper limit of the band, then

$$\omega_0 = \sqrt{\omega_L \omega_U} \quad (8)$$

On the other hand, Eq. (2) can be shown as

$$\frac{C_1}{C_2} = \frac{L_2}{L_1} = k \quad (9)$$

Using Eqs. (5), (7)-(9), we obtain that the upper limit of the band is

$$f_u = \frac{1 + \sqrt{1 + \frac{1}{k}}}{2} \frac{1}{\pi \sqrt{L_1 C_2}} = b f_c \quad (10)$$

As known, f_c given in Eq. (1) is the cutoff frequency of a LP-DA. Therefore, b is the ratio of the upper limits of the BP-DA and LP-DA. On the other hand, if the aimed ratio of the upper limits of the DAs is b , then

$$k = \frac{C_1}{C_2} = \frac{L_2}{L_1} = \frac{1}{4(b^2 - b)} \quad (11)$$

can be used to obtain values of C_1 and L_2 .

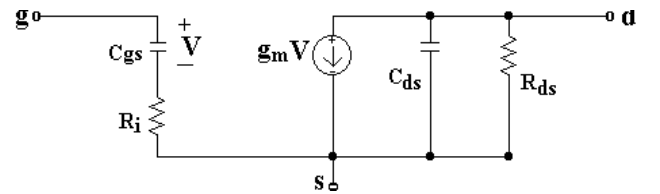


Figure .4 Simplified small signal FET model used in the simulations

One of the important problems in a DA is the input parasitic resistance R_i of the transistors. The simplified model of a FET including R_i is illustrated in Figure 4. R_i causes a shunt conductance at the input of the active component, which increases rapidly with frequency. The

shunt conductance in the gate-line can be approximated as

$$G_i \cong \omega^2 C_{gs}^2 R_i \quad (12)$$

for each transistor [4]. Therefore, the upper frequency limit of a conventional DA is always lower than the cut-off frequency (f_c) of the artificial line [3].

It is clear that the gate-line loading also exists in a DA with BP filter structure [6]. Therefore, a big peaking at the lower limit of the frequency band occurs in BP-DA; the input resistance R_i causes the gain to decrease in the upper region of the band. On the other hand, there are not damping resistances of the shunt inductances, which cause gain to decrease in the lower region of the frequency band. Therefore, the damping resistances (R_b) can be used to suppress the peaking. In case of $R_b \cong R_i$, the effect of R_b on the gain in the lower region is almost the same as that of R_i in the upper region.

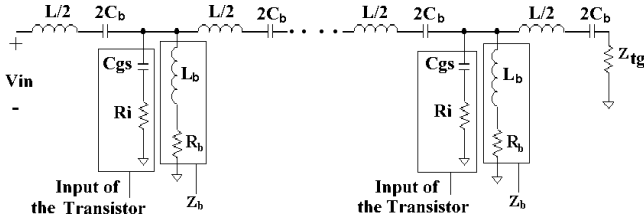


Figure.5 The gate-line of the improved BP-DA

Gate-line of the improved BP-DA is shown in Figure 5. Like R_i , the damping resistance causes a shunt conductance in the gate-line. As a result, the shunt conductance is approximately obtained as

$$G_2 \cong \frac{R_b}{\omega^2 L_b^2} \quad (13)$$

As explained above, the phase shift per BP section is zero at the center frequency. If the number of transistors is n , then the total conductance's in the gate and drain lines at the center frequency will be, respectively,

$$G_{gT} = \frac{I}{R_{gT}} \cong \frac{n(R_i + R_b)}{Z_0^2 k} \quad (14)$$

$$G_{dT} = \frac{I}{R_{dT}} = \frac{n}{R_{ds}} \quad (15)$$

We can easily obtain the voltage gain from the source to the gate-line using Eq. (14) and the voltage gain from the gate-line to the load using Eq (15);

$$A_1 \cong \frac{Z_{tg} // R_{gT}}{Z_{tg} // R_{gT} + Z_g} \quad (16a)$$

$$A_2 \cong -ng_m (R_{dT} // Z_{td} // Z_L) \quad (16b)$$

In Eq. (16a) Z_{tg} is the termination resistance of the gate-line and Z_g is the source resistance. In Eq (16b) Z_{td} is the termination resistance of the drain-line and Z_L is the load resistance. If $Z_g=Z_L$ and both are real, it can be easily shown that S_{21} of the BP-DA is

$$S_{21} = 2 \frac{V_o}{V_g} = 2 A_1 A_2 \quad (17)$$

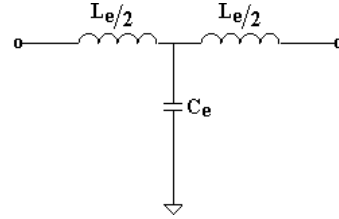


Figure.6 A lowpass T section

As mentioned above, the phase shift per BP section is zero at the center frequency. In that case, the shunt conductances at the input and output of the transistors appear in parallel and Eqs. (14) and (15) are obtained. Therefore R_i , R_b and R_{ds} cause the gain of the BP-DA to decrease and to show a minimum at the center frequency (this gain can be calculated by using Eqs. (16) and (17)). The decrease in the gain can be reduced if the phase differences between signals of neighbouring transistors are made non-zero at the center frequency. Inserting lowpass T sections into the artificial BP lines, we can achieve this, since an LP-T section has a non-zero phase difference for non-zero frequencies. In this way, the summing of the shunt conductances can be avoided. This helps the gain to increase at the center frequency. Figure 6 shows an LP-T section [4]. The characteristic impedance of the T section should be the same as that of the artificial lines, i.e.

$$\sqrt{\frac{L_e}{C_e}} = Z_0 \quad (18)$$

and its cut-off frequency should be equal to or higher than the upper frequency limit of the BP-DA, i.e.

$$\frac{1}{\pi \sqrt{L_e C_e}} \geq f_u \quad (19)$$

The characteristic impedance change of the LP-T section versus frequency is not the same as that of the BP section. This may be cause the performance of the BP-DA to deteriorate. Therefore, we must decide on the number of T sections to be used and where to insert these sections. Our investigations show that using two lowpass T sections and inserting them between the transistors in the middle give the best performance improvement. Figure 7 below shows the schematic diagram of the proposed BP-DA.

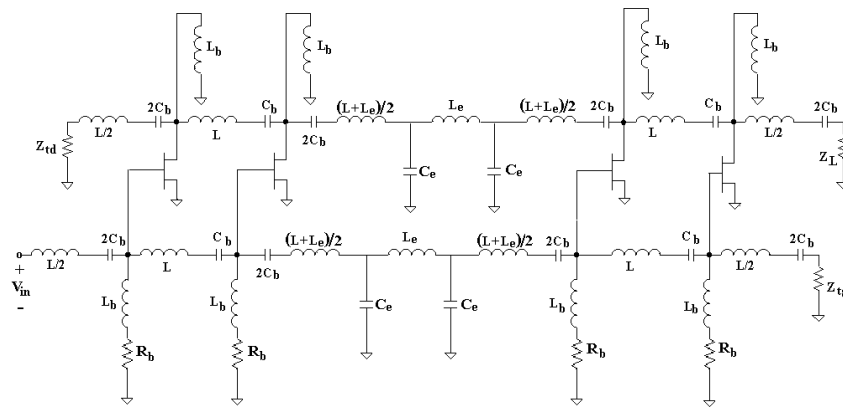


Figure.7 The proposed BP-DA with extra LP-T sections and damping resistances R_b

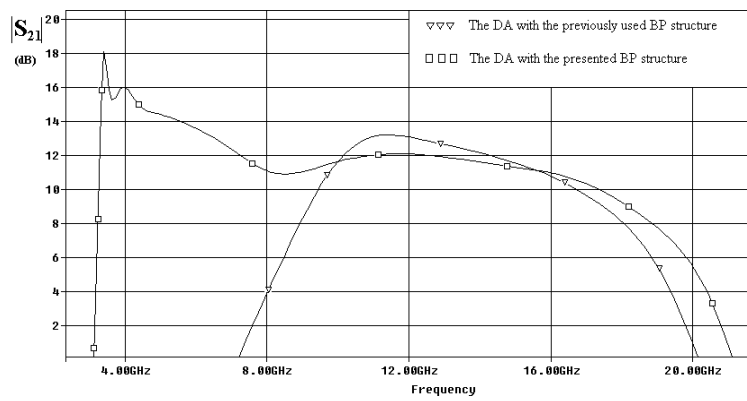


Figure.8 The gain-frequency characteristics of the BP structures

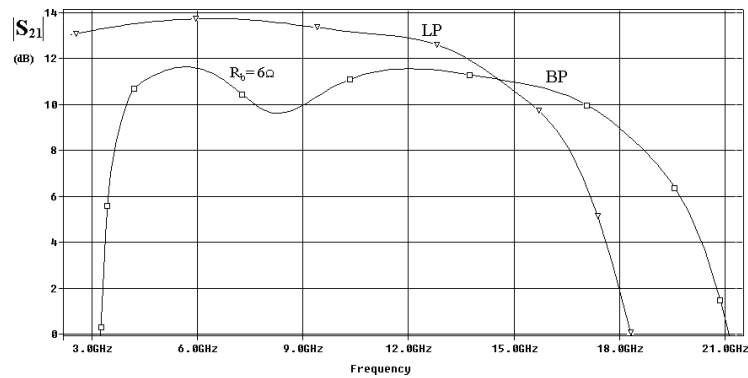


Figure.9 Gain-frequency characteristics of the BP-DA improved by R_b and LP-DA

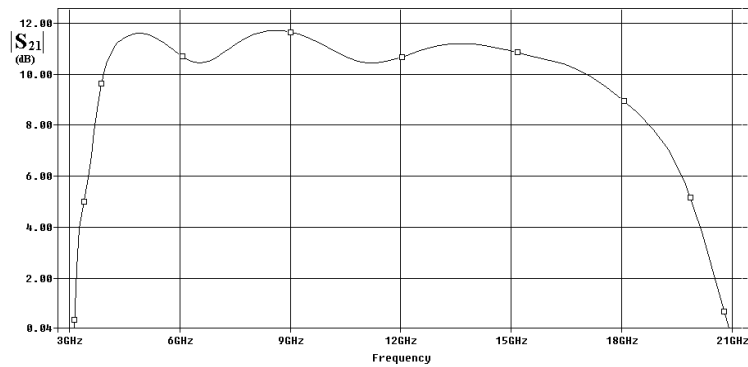


Figure.10 Frequency response of the proposed BP-DA

IV. SIMULATION RESULTS AND DISCUSSION

The small signal FET model used in simulations is illustrated in Figure 4. The DAs used in the simulations consist of four transistors. Element values of the model have been extracted from measurements of a commercially available 300- μm GaAs MESFET. The values are $C_{gs}=0.35\text{pF}$, $C_{ds}=0.14\text{pF}$, $R_i=6\Omega$, $R_{ds}=1500\Omega$ and $g_m=70\text{mS}$. As seen, C_{ds} is smaller than C_{gs} . In practice, the characteristic impedances and the delays of the input and output lines are aimed to be equal. Therefore, an extra capacitance is used to satisfy $C_{ds}=C_{gs}$. Figure 8 shows the gain-frequency characteristics of the previous and proposed BP structures. For this simulation, element values are $L=0.875\text{nH}$, $C_b=0.42\text{F}$ ve $L_b=1.05\text{nH}$. and $C_b/C_{gs}=L_b/L=1.2$ has been chosen. It is clear that L must be 0.875nH for $Z_0=\sqrt{L/C_{gs}}=50\Omega$. As can be observed from Figure 8, the bandwidth of the DA with the previously used BP structure is lower than that of the DA with the BP structure used in this work.

It can be observed from Figure 8 that there is a large peaking at the lower limit of the frequency band of the DA with the proposed BP structure. As mentioned above, the peaking can be suppressed by means of damping resistances of the shunt inductors in the gate line. Figure 9 shows the gain frequency characteristics of the BP-DA with 6Ω damping resistances and the LP-DA. It is clear from Figure 9 that the damping resistances improve the gain-frequency characteristic. The gain of the BP-DA is $\sim 11\text{dB}$ which is $\sim 2\text{dB}$ lower than that of the LP-DA. It can be observed from the figure that the bandwidth of the BP-DA is $\sim 14.5\text{GHz}$. This is approximately equal to that of the LP-DA ($\sim 15\text{GHz}$). Figure 9 is also convenient for examining the formulas given for the upper frequency limit and the gain at the center frequency. $k=1.2$ has been chosen for the BP-DA. Then b is approximately calculated as 1.177 . The simulation results give the upper frequency limit of the LP-DA as 14.95GHz and that of the BP-DA as 18.25GHz . Thus, $b \cong 1.22$ is obtained at the end of the simulations. The reason of the difference is that Eq.(10) has been obtained for $R_i=0$ and simulations have been carried out for $R_i=6$. On the other hand, using Eqs.(16) and (17) given for gain, we calculate $|S_{21}|$ as 9.63 dB at the center frequency ($\omega_0=8.3\text{GHz}$). As a result, the calculated value is approximately equal to the value obtained by the simulation and the average value of $|S_{21}|$ is approximately 1 dB higher.

It is clear from Figure 9 that the gain of the BP-DA decreases at the center frequency. To reduce the decrease in the gain, two lowpass T sections have been used. The proposed BP-DA is illustrated in Figure 7. $R_b=5.25\Omega$ has been chosen to obtain the best performance. The T sections have been inserted between the second and third transistors. The gain-frequency characteristic of the proposed BP-DA is illustrated in Figure 10. The T sections have caused ripples in the frequency band because the characteristic impedance change of the T

section versus frequency is not the same as that of the BP sections. The maximum ripple in the gain-frequency characteristic of the proposed BP-DA is 1.26dB . The ripple in the gain-frequency characteristic of the BP-DA without the T sections is 2 dB . Thus, the maximum ripple has been reduced by $\sim 0.75\text{dB}$. It can be seen from Figure 9 and 10 that the average value of $|S_{21}|$ and the bandwidth have not changed.

Another important point for a DA is phase response. The phase response of the BP-DA is approximately linear within the pass-band. But, the linearity deteriorates in the lower region of the band. The reason is that the BP structure shows highpass behaviour in this region (One can see the same point by investigating Eq (4) given for γ). It may be useful to take this point into account for applications of the BP-DA.

V. CONCLUSION

In this work, a DA with BP filter structure is presented to shift the frequency band of operation of a distributed amplifier and analysed by means of a distributed bandpass transmission line model. The basic analysis has been made and formulas of the gain and upper frequency limit have been given. Then, methods have been introduced in order to improve the gain-frequency behaviour. The basic design of a DA with the BP structure can be made by means of the formulas and methods given in this paper. Consequently, it has been shown that, despite the lower gain, the BP-DA improved by the methods is a good way to increase the maximum frequency of operation of a DA for applications not requiring DC operation.

REFERENCES

1. W. S. Percival, British Patent Specification No.460, 562, 1936
2. Y. Ayasli, S. W. Miller, R. Mozzi and L.K. Hannes, "Capacitively Coupled Travelling-Wave Power Amplifier", IEEE Trans. Microwave Theory Tech., vol. MTT-32, Dec. 1984, pp. 1704-1709
3. J. B. Beyer, S. N. Prasad and R. C. Becker, "MESFET distributed amplifier guidelines", IEEE Trans. Microwave Theory Tech., vol. MTT-32, Mar. 1984, pp. 268-275
4. T. T. Y. Wong, Fundamentals of Distributed Amplifiers, Artech House, Boston, 1993
5. B. J. Minnis, "Extending the frequency range of distributed amplifiers with bandpass filter structures", Microwave J., vol. 33, 1989, pp 109-122
6. M. Yazgi, A. Toker, D. Leblebici, "On Distributed Amplifiers with Bandpass Filter Structure", Proceedings of ELECO'99, International Conference on Electrical and Electronics Engineering, Bursa, Turkey, December 1999, pp. 128-1317
7. F. R. Connor, Wave Transmission, Edward Arnold (Publishers) Ltd., London, 1972
8. K. L. Su, Analog Filters, Chapman & Hall, London, 1996